

Super-resolution imaging of SERS hot spots

Q1 Q2

Katherine A. Willets

Cite this: DOI: 10.1039/c3cs60334b

Surface-enhanced Raman scattering (SERS) hot spots occur when molecules are positioned near regions of strongly enhanced electromagnetic fields on the surface of nano-featured plasmonic substrates. The emission from the molecule is coupled out into the far field by the plasmon modes of the substrate, but due to the diffraction-limit of light, the properties of this coupled molecule-plasmon emitter cannot be resolved using typical far-field optical microscopy techniques. However, by fitting the emission to a model function such as 2-dimensional Gaussian, the relative position of the emitter can be determined with precision better than 5 nm in a process known as super-resolution imaging. This tutorial review describes the basic principles of super-resolution imaging of SERS hot spots using single molecules to probe local electromagnetic field enhancements. New advances using dipole-based fitting functions and spectrally- and spatially-resolved measurements are described, providing new insight into SERS hot spots and the important roles of both the molecule and the substrate in defining their properties.

Received 20th September 2013

DOI: 10.1039/c3cs60334b

www.rsc.org/csr
Key learning points

- (1) Super-resolution imaging allows local SERS signal enhancements due to plasmon-enhanced electromagnetic fields (*e.g.* hot spots) to be explored with spatial resolution on the order of 1–10 nm.
- (2) The location of SERS emission is calculated by fitting diffraction-limited emission to a model function, such as a 2-dimensional Gaussian or a sum of multiple dipole emitters, to determine the emission centroid.
- (3) The spatial origin of SERS is a convolution between the position of the molecule on the substrate surface and the radiating plasmon modes of the substrate.
- (4) Successful super-resolution SERS hot spot imaging requires working at or near the single molecule limit.
- (5) Molecular motion in and out of an electromagnetic hot spot changes the coupling between the SERS emitter and the plasmon modes of the substrate, thereby shifting both the calculated centroid and affecting the measured SERS intensity.

1. Introduction

Surface-enhanced Raman scattering (SERS) has generated significant interest as an analytical spectroscopy technique due to its molecular specificity (based on measuring vibrational modes of a molecule) and high sensitivity (down to the single molecule level).^{1–3} In SERS, normally weak Raman signals are enhanced by up to nine orders of magnitude by placing an analyte of interest on or near a nanoscale-roughened noble metal surface. The enhancement in the SERS signal is due to a combination of two effects: enhanced electromagnetic (EM) fields at the substrate surface, known as the EM enhancement effect, and chemical interactions between the molecule and the noble metal substrate, known as the chemical enhancement effect.⁴ The EM enhancement effect is recognized to dominate SERS enhancement and is due to the excitation of localized surface plasmons within the noble metal substrate.⁵ Localized surface plasmons are light-driven collective oscillations

of the surface conduction electrons in a material with a negative real and small positive imaginary dielectric constant. This dielectric condition is met by noble metals such as gold and silver in the visible and near-infrared region of the EM spectrum.⁶ As a result, the bulk of SERS experiments are conducted on gold and silver substrates, although other metals, such as aluminum and platinum, have also been used.⁷ Because excitation of localized surface plasmons requires that the surface conduction electrons oscillate in concert as they are driven by the electric field of the excitation light, SERS substrates must have features that are smaller than the wavelength of light, which is typically achieved by using nanostructured thin films or nanoparticles as SERS substrates.^{8,9}

A number of measurement tools have been used to characterize both SERS signals and the substrates that support SERS including Raman spectroscopy and microscopy, dark-field scattering, near-field scanning optical microscopy (NSOM), atomic force microscopy (AFM), and electron microscopy and spectroscopy.^{10–12} In particular, a great deal of attention has

Department of Chemistry, University of Texas at Austin, 102 E. 24th St. STOP A5500, Austin, TX 78712, USA. E-mail: kwillets@cm.utexas.edu

1 been paid to EM “hot spots” within SERS substrates, which
are nanoscale regions of the SERS substrate that have the
strongest local EM field enhancement.^{13,14} The simplest
model of an EM hot spot is the junction or gap region between
5 two adjacent nanoparticles in a nanoparticle dimer; theory
predicts that EM field intensities can be enhanced by as
much as 10^7 in the gaps relative to the incident intensity.¹⁴
Characterizing hot spots has proven a distinct experimental
challenge because the size of the hot spot ($\sim 1\text{--}10$ nm) is well
10 below the optical diffraction limit, which prevents objects
smaller than roughly half the wavelength of light from being
resolved in an optical microscope.¹⁵ As a result, SERS emis-
sion coupled to EM hot spots cannot be resolved beyond the
200–400 nm length scale, which is well above the relevant
15 length scale of the hot spots.¹⁶

Starting in 2010, several groups have sought to overcome
this fundamental optical resolution limit by applying a techni-
que known as super-resolution imaging to study hot spots with
<10 nm resolution.^{17–21} Super-resolution imaging is some-
thing of an umbrella term, encompassing several different
20 forms of far-field optical microscopy that provide sub-
diffraction limited imaging resolution (NSOM is considered a
separate form of optical imaging, given that it achieves sub-
diffraction-limited resolution through near-field excitation).²²
For the purpose of this Tutorial Review, we will use super-
25 resolution imaging to describe a strategy in which diffraction-
limited optical images are fit to some model function in order
to calculate the position of the emitter with precision of $\sim 1\text{--}$
10 nm.²³ This approach is inherently single molecule in nature,
because it requires that only a single emitter be active at a given
30 time, such that its position can be uniquely determined.²³
Other sub-diffraction-limited far-field imaging techniques,
such as stimulated emission depletion or structured illumina-
tion microscopy, use modified excitation sources to achieve
improved optical resolution and are therefore thematically
35 distinct from the technique described here.²² Tip-enhanced
Raman scattering (or TERS) is another method for sub-
diffraction-limited resolution and is capable of single molecule
sensitivity, but achieves enhancement through the use of a
sharpened metallic tip to create sub-wavelength EM hot
40 spots.^{24,25} As a scanning probe technique, TERS is excellent
for surface characterization, but is also time-consuming and
not as well-suited for solution-phase measurements as
nanoparticle-based SERS substrates.

Because we have reviewed the major results of super-
resolution imaging of plasmonic systems elsewhere,^{15,26} this
Tutorial Review will focus on describing the experimental
considerations required for successful super-resolution SERS
imaging experiments, while highlighting some of the most
50 recent advances in the field based on new fitting func-
tions for modeling diffraction-limited spots and spectrally-
and spatially-resolved hot spot imaging. Although our focus
is primarily on hot spots for SERS spectroscopy, experiments
using both Raman scattering and fluorescence readouts will
55 be described in order to provide a more complete description
of the current state-of-the-art approaches within the field.

2. Basic principles of super-resolution imaging

For the purpose of this review, we will assume that the reader is
familiar with basic forms of microscopy; we refer the interested
reader elsewhere for a more in-depth discussion of different
microscopy techniques.²⁷ Most super-resolution imaging
experiments are performed in a wide-field geometry, such that
a large field of view is illuminated on the sample allowing for
multiple emitters to be interrogated simultaneously. Fig. 1 shows
10 a representative block diagram of wide-field epi-illumination
using an inverted microscope; other geometries based on
upright microscopes or total internal reflection will also work
for these studies. The critical component is that in a single
image, individual emitters are spaced by more than the
15 diffraction-limit of light, such that each can be uniquely
resolved as a single diffraction-limited spot on a 2-dimensional
(2-D) detector, as shown in Fig. 1.

While scanning confocal microscopy can also produce
diffraction-limited images of individual emitters, wide-field
imaging using a 2-D CCD detector is favored for super-
resolution studies, because it allows large regions of interest
to be interrogated simultaneously. This is especially important
if there are any dynamic processes occurring, such that the

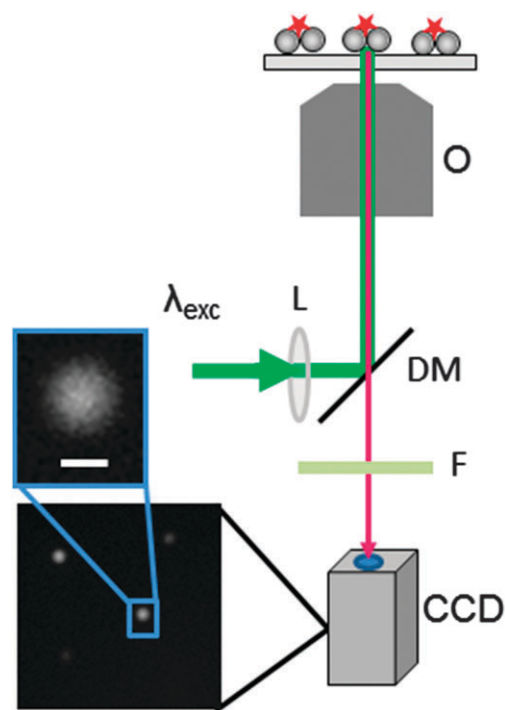


Fig. 1 Block diagram of an inverted microscope used for SERS super-resolution imaging. Excitation light (green line) is passed through a lens (L) at the back focal plane of the objective, then reflected off a dichroic mirror (DM) and passed through a microscope objective (O), producing a wide-field excitation spot at the sample plane. SERS from the sample (pink line) is collected back through the objective and appropriately filtered (F) to remove Rayleigh scattered light, before being imaged onto a CCD camera. Emission from individual SERS-active nanoparticles appear as diffraction-limited spots (blue box). Scale bar = 500 nm.

1 location of the emitter is changing with time; such dynamics
 cannot be captured by a scanning technique that builds up a
 diffraction-limited image pixel-by-pixel. Because a 2-D detector
 is used for these studies, a critical experimental consideration
 5 is the size of the CCD imaging pixels relative to the size of the
 diffraction-limited spot.²⁸ Fig. 2 shows a representative
 diffraction-limited Airy disk (Fig. 2A) projected onto hypothetical
 2-D detectors with varying pixel size. For this simulation, the
 emitter produced 5000 photons (N) with a wavelength of 540 nm,
 10 and an objective with a numerical aperture (NA) of 1.4 was used
 for both illumination and collection. Normally-distributed noise
 was added with a standard deviation of \sqrt{N} to simulate the shot
 noise limit under high photon counts (a reasonable approxi-
 mation for this purely illustrative calculation). In the case when
 15 the pixel size of the detector is too small relative to the size of the
 Airy disk (Fig. 2B), too few photons are captured by each pixel,
 and the peak shape of the diffraction-limited emitter is obscured

by the noise. On the other hand, if the pixel size is too large
 relative to the Airy disk (Fig. 2D), the photons are distributed
 over too few pixels and the shape of the peak is lost. Webb and
 coworkers have calculated that the ideal detector pixel size for
 measuring and then fitting diffraction-limited emission is
 5 roughly the size of the standard deviation of the point spread
 function of the spot, which is about one third of the Airy disk
 radius (Fig. 2C).²⁸

Having described the major experimental considerations,
 we next turn to the heart of super-resolution imaging: fitting a
 10 diffraction-limited spot to some model function in order to
 calculate the (approximate) location of the emitter with preci-
 sion below 10 nm. The simplest function to use is a 2-D
 Gaussian, given by eqn (1) below:

$$I(x, y) = z_0 + I_0 \exp \left[-\frac{1}{2} \left[\left(\frac{x - x_{0G}}{s_x} \right)^2 + \left(\frac{y - y_{0G}}{s_y} \right)^2 \right] \right] \quad (1)$$

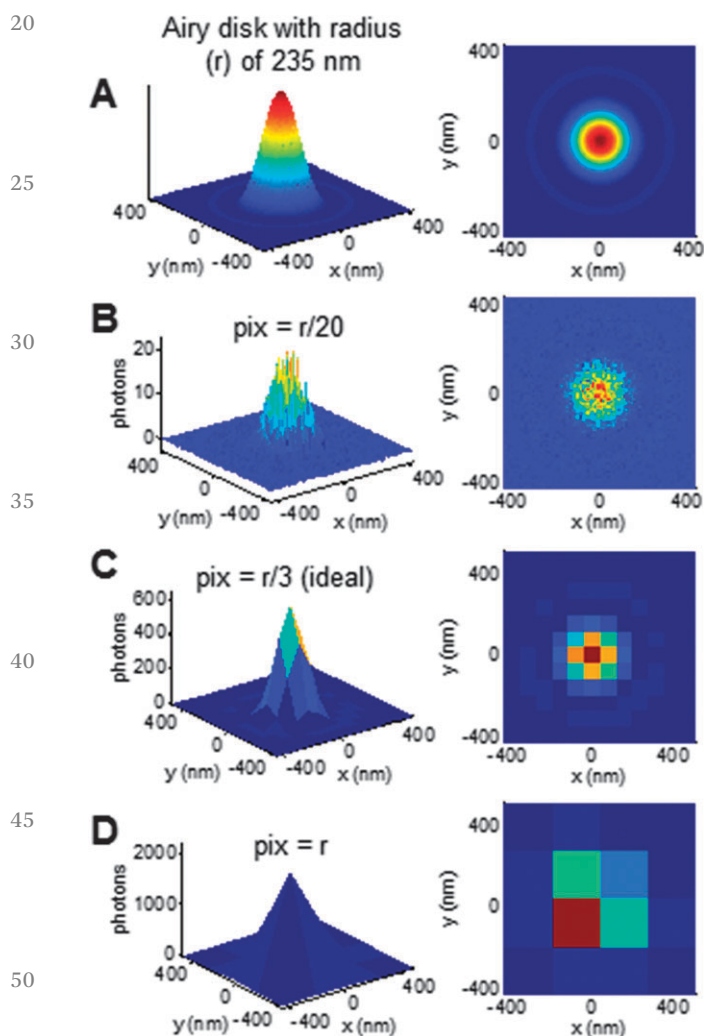


Fig. 2 (A) Calculated Airy disk pattern for 540 nm light collected through a 1.4 NA lens. (left) 3-D view, (right) 2-D projection. (B–D) Projection of the Airy disk from A onto a 2-D detector with different pixel sizes (pix) relative to the radius (r) of the Airy disk. Each emitter corresponds to 5000 photons with normally distributed noise.

In this equation, $I(x, y)$ represents the intensity of the
 diffraction-limited emitter spread over the imaging pixels of
 the detector, z_0 is the intensity of the background, I_0 is the peak
 intensity, x_{0G} and y_{0G} are the centroid position of the Gaussian
 (e.g. the position of peak intensity), and s_x and s_y are the
 standard deviations of the Gaussian in x and y , respectively.
 The position of the emitter is approximated as the centroid
 position of the 2-D Gaussian. The appropriateness of this
 model function to describe SERS emission will be discussed
 in more detail in Section 4, but the advantages of the 2-D
 Gaussian model are the robustness of the model, the small
 number of fitting parameters (six) and the low computational
 cost. As a result, the 2-D Gaussian is the most popular option
 for fitting diffraction-limited emission. Importantly, by fitting
 the diffraction-limited emission to a 2-D Gaussian, the position
 of the centroid can be determined with precision that is
 typically better than 10 nm depending on the number of
 emitted photons, the standard deviation of the background,
 the width of the Gaussian, and the pixel size of the detector.²⁸
 Under the approximation that the calculated centroid repre-
 sents the position of the emitter, this means that its location
 is known with a precision that is over an order of magnitude
 better than the diffraction-limit, well within the relevant length
 scale of EM hot spots.

One challenge with using this fitting approach to determine
 the location of an emitter is that it requires that only a single
 species be emitting at a time within a diffraction-limited spot.
 If two emitters are spaced by less than the diffraction limit,
 their emission will be super-imposed and their positions cannot
 be uniquely resolved; put another way, the calculated centroid
 will be an intensity-weighted super-position of the locations of
 the two individual emitters. Thus, it is critical to control the
 emission in such a way that only a single species is active
 within a diffraction-limited spot at a given time.²³ Strategies
 for achieving this in super-resolution fluorescence imaging are
 beyond the scope of this review, but for SERS hot spot imaging,
 we must work in the single molecule limit—that is, only a
 single molecule can occupy an EM hot spot at a time. To date,

1 this has been achieved *via* diffusion of molecules in and out the
hot spot, providing a simple mechanism for ensuring that only
a single emitter is active at a time and that the calculated
centroid position has some fundamental correlation with the
5 position of the emitter.^{17–21,29} Section 3 will discuss this
principle in more detail by showing examples comparing SERS
super-resolution imaging in the single- and multi-molecule
regimes.

A final important consideration for super-resolution imaging
10 experiments is sample drift. Typical super-resolution imaging
experiments involve the acquisition of many sequential images,
so the position of individual emitters can be followed over time.
Because super-resolution fits yield centroid positions with pre-
15 cision better than 10 nm, any nanoscale change in the position
of the sample relative to the microscope will yield a measurable
change in the calculated centroid. Given that most samples are
mounted on mechanical translation stages, allowing different
regions of a sample to be studied, experimenters must compen-
20 sate for any stage drift that occurs over the course of the
experiment as the gears of the translation stage settle with
time. The most straightforward way to achieve this is to include
fixed-position alignment markers in the sample, which provide
stable emission signals that are used to correct for stage drift. A
25 simple example of alignment markers are fluorophore-doped
polystyrene spheres, which provide diffraction-limited emission
that can be fit to a 2-D Gaussian and their calculated centroid
position used to calculate the magnitude of the drift as a func-
tion of time. Including stage drift corrections is critical for
successful super-resolution imaging studies in order to verify
30 that changes in the calculated centroid positions are real effects
associated with the sample under study, rather than spurious
effects due to mechanical instabilities.

35 3. Mapping SERS hot spots with super-resolution imaging

As a first example of super-resolution imaging of SERS hot
spots, we will consider work from our group in which a single
Rhodamine 6G (R6G) molecule is adsorbed to a silver nano-
40 particle aggregate (as shown in the cartoon in Fig. 1).¹⁷ Working
at the single molecule SERS (SM-SERS) level removes the
probability that multiple molecules are contributing to the
measured SERS signal, allowing us to correlate the location of
the single SERS emitter with the calculated centroid position.
One major challenge in these experiments is that silver (and
45 gold) nanoparticles show single photon luminescence under
blue/green excitation; thus, we have two emission sources: the
luminescence from the aggregated silver nanoparticles and the
SERS emission associated with the R6G.²⁰ The cross-section of
the luminescence is sufficiently weak that the SERS can easily
50 be observed above this background, but for completeness, it is
important to remove the contribution from the silver in order
to isolate the SERS signal. To do this, we exploit the inherent
on/off intensity fluctuations associated with SM-SERS, which
55 are believed to occur when the molecule diffuses in and out of

the hot spot.² Times associated with SERS emission are identi-
fied by large jumps in the detected intensity above the stable
background, although in later work, we introduced spectral
correlation to unambiguously assign emission as originating
5 from SERS.¹⁹ During times when the molecule is not in the hot
spot, we can fit the diffraction-limited emission from the silver
nanoparticle luminescence alone and determine its spatial
origin.¹⁷ Then, when the molecule diffuses into the hot spot,
we can subtract the known contribution from the nanoparticle
10 luminescence away from the measured emission, leaving us
with the contribution from the R6G SERS.

Fig. 3A shows an example of the centroid positions deter-
mined from 800 individual image frames of data.¹⁷ For frames
in which only silver luminescence is observed, the calculated
centroids are shown as black circles; these data are symmetri-
15 cally distributed around a mean value (arbitrarily set to zero in
both *x* and *y*) with a standard deviation of ~ 8 nm, which is
roughly the calculated precision based on the low signal-to-
noise of the luminescence. For the frames in which R6G SERS is
observed, the calculated centroid data (after the removal of the
20 silver luminescence contribution) are shown in red. Unlike the
luminescence data, the SERS centroids are asymmetrically
distributed and extend over a >20 nm region, much larger than
our expected precision based on the high signal-to-noise of the

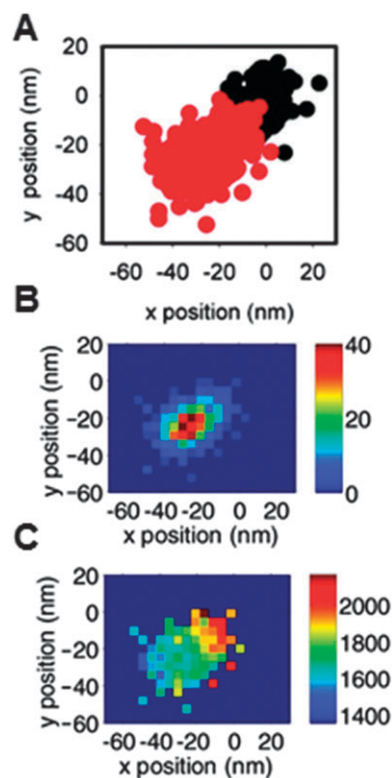


Fig. 3 (A) Centroid positions calculated for (black) silver luminescence and (red) SERS emission from a SM-SERS active nanoparticle aggregate. (B) Frequency histogram showing the number of SERS centroid positions located within each bin. Bin size is 4.6 nm. (C) Spatial intensity map showing the average SERS intensity of all points in each bin. Adapted with permission from ref. 17. Copyright 2010 American Chemical Society.

1 SERS signal. To better represent these data, we calculate 2-D
2 histograms, in which we count the number of centroids that fall
3 into spatially-defined bins, rejecting any with poor quality
4 (based on the R^2 value) of the fit. The resulting frequency
5 histogram is shown in Fig. 3B and reveals that the asymmetric
6 shape and extended area of the SERS centroid positions is
7 preserved. Next, we calculate the average SERS intensity of all
8 points within each bin of the frequency histogram and plot this
9 as a spatial intensity map, shown in Fig. 3C. The spatial
10 intensity map shows that SERS centroids located closest to the
11 average luminescence centroid are associated with the strongest
12 SERS intensity and that the intensity decays in a directional,
13 gradient fashion as the centroid position moves away from this
14 highest intensity spot. This SERS intensity profile is consistent with
15 theoretical calculations, which show that plasmon-enhanced EM
16 fields are typically most strongly enhanced in the region between
17 two adjacent nanoparticles, while decaying in gradient fashion as a
18 function of distance from the junction region.¹⁴ Thus, the spatial
19 intensity map is a reflection of the SERS hot spot, as reported by a
20 single molecule.

21 In these experiments, the position of the SERS emission
22 does not reflect the absolute position of the emitter, but is
23 instead a convolution between the position of the molecule and
24 the plasmon modes of the underlying nanostructure.^{17,30} Based
25 on the position of the molecule on the nanoparticle surface, the
26 coupling between the emitting dipole and the plasmon modes
27 can change, which changes how the emission is coupled into
28 the far field by the plasmonic nanoantenna.³⁰ Earlier, we
29 introduced the idea that the molecule may be diffusing in
30 and out of the hot spot, leading to intensity fluctuations in
31 the SM-SERS signal. Molecular diffusion is also the mechanism
32 believed to be responsible for the changing position of the
33 calculated SERS centroid. Thus far, we have defined the EM hot
34 spot as the region on a SERS substrate associated with the
35 strongest EM field enhancement. However, the EM field
36 enhancement is due to the excitation of localized surface
37 plasmons, and with nanoparticle aggregates, there are multiple
38 plasmon modes that can be excited. For example, the dipole
39 plasmon associated with the long axis of a nanoparticle dimer
40 (the longitudinal mode) will yield the highest calculated EM
41 field enhancement, but smaller contributions due to the dipole
42 plasmon mode aligned with the short axis of the dimer (the
43 transverse mode), and even quadrupole modes, can be
44 excited.³¹ If we now consider Raman scattering from a mobile
45 molecule on the nanoparticle surface, the emission will couple
46 into these different plasmon modes with varying efficiency,
47 depending on the position of the molecule and its ability to
48 excite the different plasmon modes.³⁰ The result is that the
49 centroid position of the SERS emission will change as the
50 position of the molecule changes, impacting how its emission
51 is re-radiated into the far field by the plasmonic substrate.¹⁷ Put
52 another way, while the EM hot spot is defined exclusively by
53 how the excitation leads to local EM field enhancements on the
54 nanoparticle surface, the SERS hot spot is a convolution
55 between the plasmon-enhanced EM fields and the position of
56 the coupled molecular emitter on the surface.

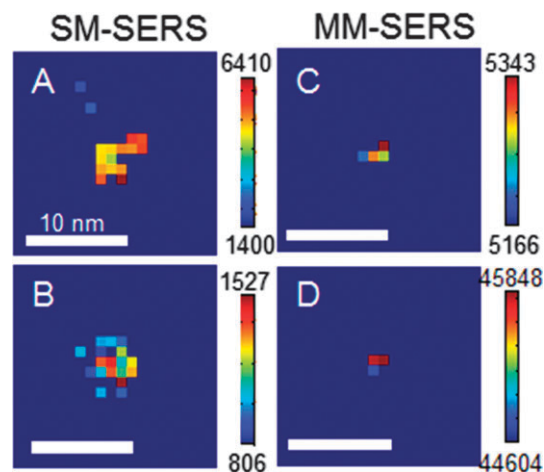


Fig. 4 Spatial intensity maps for SERS active nanoparticle dimers in the (A and B) single molecule and (C and D) multiple molecule limits. Adapted with permission from ref. 30. Copyright 2013 American Chemical Society.

21 To further illustrate this idea, Fig. 4 compares the spatial
22 intensity maps from nanoparticle dimers labeled with either
23 ~ 1 R6G molecule (SM-SERS, Fig. 4A and B) or ~ 100 R6G
24 molecules (multi-molecule, or MM-SERS, Fig. 4C and D).³² In
25 the case of the SM-SERS examples, variation in the centroid
26 position and SERS intensity is observed as the single R6G
27 molecule moves over the nanoparticle surface, changing how
28 the molecular emission couples to the different plasmon
29 modes of the dimer. On the other hand, in the MM-SERS case,
30 the centroid position is extremely stable with a calculated
31 precision of < 0.5 nm in both cases. Moreover, the intensity
32 varies by less than 5% in the MM-SERS case, unlike the SM-SERS
33 case where the intensity varies by roughly a factor of two or more.

34 Earlier, we described the idea that if multiple emitters are
35 active at the same time, the calculated centroid is an intensity-
36 weighted super-position of their positions. In the MM-SERS
37 regime, the molecular coverage is sufficiently high that all
38 resonant plasmon modes of the nanostructure are coupled to
39 SERS emission, leading to a collapse of the centroid position
40 to a single average value. Thus, we lose all dynamics associated
41 with the molecules on the surface and are no longer able to map
42 out the SERS hot spot. These data illustrate the importance of
43 working at or near the single molecule regime in order to provide
44 useful super-resolution imaging data and map out hot spots with
45 < 10 nm resolution.

46 Other groups have exploited solution phase diffusion to
47 control the reporter concentration and map out EM hot spots,
48 using fluorescence as an optical read-out rather than Raman
49 scattering.^{18,29} For these studies, plasmonic substrates are
50 imaged in a dilute solution of fluorescent dye molecules. When
51 a single fluorophore gets close enough to a hot spot, the
52 emission is enhanced and recorded as a single diffraction-
53 limited burst of fluorescence on the CCD detector. The fluoro-
54 phore then photobleaches (*e.g.* stops emitting) or diffuses
55 away, and no emission is recorded until another fluorophore
56 diffuses close enough to the hot spot, thereby allowing the process to
57 be repeated. Much like the SERS data described above, a resulting

map of the fluorescence intensity as a function of centroid position can be constructed. As with the SERS results, the gradient decay in intensity and extended size of the hot spot is reproduced with the fluorescence data.¹⁸ In these experiments, both nanoparticle aggregates and nanostructured thin films were studied, and sub-wavelength hot spot dimensions were observed for both substrates.^{18,29} Thus, defeating the diffraction limit through super-resolution techniques is critical in order to observe the spatial and intensity variation of molecular emission coupled to EM hot spots in plasmonic substrates.

4. Fitting diffraction-limited SERS emission: going beyond the Gaussian approximation

In Section 2, we introduced the concept of fitting diffraction-limited spots to a model function and stated that a 2-D Gaussian was the most popular model in the literature for calculating the centroid position. However, the 2-D Gaussian is an approximation and does not connect to any real physics associated with the SERS emission process; rather it is a convenient model for describing the symmetric peak shape of a typical diffraction-limited image. Given that the Gaussian is a non-physical model, the earlier assumption that the center of peak intensity (*e.g.* the centroid) of the 2-D Gaussian represents the location of the emitter is useful, but ultimately flawed. Several researchers have noted that the use of this model can introduce significant inaccuracies in localizing single molecule emission, suggesting that more robust models may be required to physically describe the SERS emission.^{33,34} For single molecule fluorescence experiments, this problem can be handled by explicitly modeling a dipole emitter near a refractive index interface (*e.g.* the sample–substrate interface) accounting for the 3-dimensional (3-D) orientation of the emitter, the emission wavelength, the local refractive indices, and various other experimental parameters.^{33,35} Because the centroid in this dipole model (x_{0d} , y_{0d}) represents the position of the dipole emitter rather than the position of peak intensity (as in the 2-D Gaussian), the localization accuracy improves significantly—although at the price of increased computational expense and knowledge (or fitting) of more experimental parameters.

While a single fluorescent molecule is well-described as a single emitting dipole, for SERS emission, the physical characterization of the emission is more complex. As described above, even a simple nanoparticle dimer has multiple active plasmon modes: the dominant longitudinal dipole mode, the weaker transverse dipole modes, and the even weaker quadrupole modes. Because each of these plasmon modes can couple with molecular scattering, finding an appropriate model to describe the SERS emission from even the simplest substrate is not straightforward. However, if we look at several representative diffraction-limited images, shown in Fig. 5, we see that in some cases a dipole model for SERS emission may be appropriate.^{36,37} Fig. 5A and B, shows diffraction-limited images of

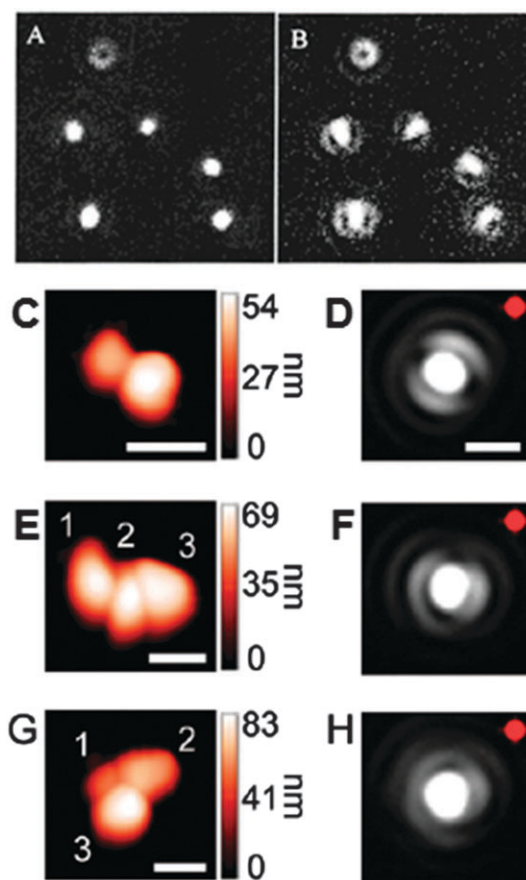


Fig. 5 (A) Focused and (B) defocused images of single molecule fluorescence. In (B), the image is defocused by 300 nm to highlight the asymmetry of dipole emission near an interface. Reproduced with permission from ref. 35. Copyright 1999 American Chemical Society. (C) AFM and (D) SERS emission from a nanoparticle dimer. (E, G) AFM and (F, H) SERS emission from two different nanoparticle trimers. Nile Blue was used as a SERS tag with ~ 1 molecule per aggregate. Images were in focus but re-contrasted to highlight the inherent asymmetry of the emission. Reproduced with permission from ref. 34. Copyright 2012 American Chemical Society.

single fluorescent molecules defocused by 300 nm in Fig. 5B to highlight the deviations from an ideal Gaussian.³⁸ The bright central peak and lower intensity oriented side lobes are characteristic of a single emitting dipole near an interface. If we now look at SM-SERS emission from a nanoparticle dimer (Fig. 5C and D), we note the same bright central peak and lower intensity oriented side lobes even without defocusing the image.³⁷ The two side lobes are oriented with the long axis of the nanoparticle dimer, suggesting that—to a first approximation—modeling the SERS signal as a single dipole oriented along the longitudinal dipole plasmon mode could be appropriate. However, as the aggregation state of the SERS substrate increases, as in Fig. 5E and H, the diffraction-limited emission no longer shares qualitative features with a single fluorescent dipole, suggesting that the applicability of the dipole model may be limited as SERS substrates grow more complex and more plasmon modes are introduced.

We have tested the ability of a dipole model to fit SERS data from nanoparticle dimers, inspired by the qualitative results

1 shown in Fig. 5.³² In addition to the centroid position (x_{0d} , y_{0d}),
 5 the dipole model generates parameters associated with the 3-D
 orientation of the dipole emitter and the emission wavelength
 (among other values). The orientation values can be compared
 to the alignment of the longitudinal dipole axis based on the
 nanoparticle structure, while the emission wavelength can be
 compared to the SERS spectrum, providing a check of the
 appropriateness of the dipole model. Unfortunately, despite
 the qualitative similarities between single dipole emission
 10 (Fig. 5B) and SERS emission from a nanoparticle dimer
 (Fig. 5D), our data show that modeling the SERS emitter as a
 single dipole fails to completely describe the emission, yielding
 systematic residuals in the fits and non-physical values of
 several known experimental parameters. In particular, the
 15 calculated emission wavelength is well to the red of the actual
 SERS emission—whether in the SM-SERS or MM-SERS regi-
 me—and the calculated 3-D orientation parameters do not
 accurately describe the 3-D orientation of the nanoparticle
 dimer in the SM-SERS regime. Thus, even though the SERS
 20 emission from a nanoparticle dimer looks similar to a single
 emitting dipole by eye, a quantitative fit shows that SERS
 emission requires a more complex model to represent the data.

Recognizing that the transverse dipole modes can also play a
 role in the measured SERS emission, we expanded the dipole
 25 model as the intensity-weighted sum of three mutually ortho-
 gonal dipoles (denoted the 3-dipole fit).³² The choice of this
 3-dipole model was motivated by previous work from our group
 (and others) in which plasmon-mediated luminescence and
 scattering from gold nanorods required three mutually ortho-
 30 gonal dipoles to correctly model the diffraction-limited emis-
 sion.³⁹ In the nanorod case, while we expected the longitudi-
 nal dipole plasmon to dominate the emission, we found that
 including two additional dipoles to account for transverse
 dipole plasmon-mediated emission improved the overall quality
 35 of fit to the experimental data. For the SERS data, we also
 found that using three dipoles improved the fit quality, re-
 ducing (although not eliminating) the systematic error in the
 calculated residuals. Moreover, the 3-D orientation parameters
 show improved agreement with the orientation of the long axis
 40 of the dimer, both in the SM-SERS and MM-SERS regimes.
 However, the calculated emission wavelength remains too far
 to the red of the actual SERS spectrum, although not as far as
 the original single dipole fit. Even if we expand our parameter
 space, allowing other values to be fit—such as the distance of
 45 the emitter from the surface or the emission wavelength of the
 three individual dipole components—we never find perfect
 agreement between the measured SERS emission and the calcu-
 lated fit, suggesting that three mutually orthogonal dipoles
 is still not a sufficient physically-descriptive model. However,
 50 despite this lack of perfect agreement, the 3-dipole fit pro-
 vides a better overall quality of fit relative to the 2-D Gaus-
 sian based on reduced residuals, suggesting improved localiza-
 tion accuracy of the SERS emission.

To compare how the calculated centroid positions vary
 55 between the 2-D Gaussian and 3-dipole models, we once again
 calculated spatial intensity maps associated with the emission.³²

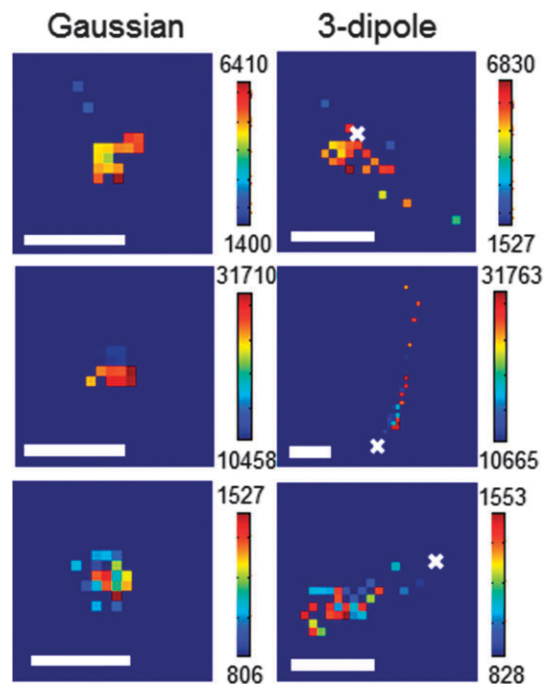


Fig. 6 Spatial intensity maps for three different SM-SERS active nanoparticle dimers, with centroids calculated using (left) a 2-D Gaussian model and (right) a 3-dipole model. For comparison, the average value of the Gaussian centroid is shown as a white "x" in the right column. All scale bars are 10 nm. Adapted with permission from ref. 30. Copyright 2013 American Chemical Society.

Fig. 6 shows three examples in the SM-SERS regime. Encouragingly, both data sets show variation in the calculated centroid positions consistent with the physical picture that motion of a single molecule on the surface changes its coupling to the various plasmon modes of the nanostructure, thereby shifting the location of the emission in the far field. However, the two spatial intensity maps are fundamentally different with the 3-dipole model showing extended areas relative to the 2-D Gaussian counterparts. Shifts in the calculated centroid for the 3-dipole case are strongly correlated with changes in the calculated out-of-plane orientation of the dimer. While this result suggests that the longitudinal dipole mode is effectively shifted out-of-plane as the molecule moves on the dimer surface, a more likely explanation is that the 3-dipole model does not completely capture the physics of the emission, given that it assumes that the three dipoles share a common origin.

The take-home message from these studies is that modeling diffraction-limited SERS emission is not as straightforward as simply assuming dominance of a single dipole plasmon mode. Even in the limit of three orthogonal dipole emitters (a vastly more computationally expensive model), the SERS emission is not completely described by the model. Herein lies the dilemma: (1) do we continue adding additional complexity—possibly by explicitly modeling plasmon modes of the underlying nanostructure based on correlated structure measurements and electrodynamics calculations—in order to fit SERS emission and obtain increasingly accurate centroid positions or (2) can

1 we rely on simpler models to provide at least a qualitative view
 into SERS hot spots and any associated dynamics?

5 The good news is that the simple Gaussian model has
 proven to yield physically reasonable results despite its non-
 physical origin, similar to results from the single-molecule
 biophysics community.^{23,40} For example, calculated spatial
 intensity maps have been compared to nanoparticle structures
 obtained by scanning electron microscopy (SEM) and have
 shown excellent agreement between the shape and orientation
 of the spatial intensity maps and the alignment of junctions
 within nanoparticle aggregates.¹⁹ Moreover, measured SERS
 and silver luminescence centroids have been compared to
 theoretical centroid values using discrete dipole approximation
 calculations and have yielded excellent agreement with experi-
 15 mentally measured values using the 2-D Gaussian model.²⁰
 Thus, the data show the merit of using the 2-D Gaussian to
 model SERS emission, despite its inherent flaws. However, the
 data also highlight the importance of understanding the phys-
 ical processes that dictate what the SERS centroid represents
 in order to correctly interpret the results.

5. Spectrally- and spatially-resolved hot spots

25 The ability to obtain simultaneous spectral and spatial infor-
 mation about SERS hot spots has several advantages, including
 identification of the Raman-active species occupying the hot
 spot as well as any wavelength-dependent properties of the hot
 spot itself. In our group, we use a 50/50 beamsplitter to split the
 SERS emission from SERS-active nanoparticles, sending half of
 the signal to a CCD camera for imaging and fitting and the
 other half to a spectrometer attached to a camera for spectral
 identification of the analyte.¹⁹⁻²¹ We used this approach to
 30 spectrally resolve two different analytes adsorbed to a single
 nanoparticle aggregate: an R6G molecule and a deuterated analog
 in which four protons on the pendant phenyl ring of the molecule
 are replaced by deuterium (R6G-d₄, Fig. 7A).²¹ Because of this substitution,
 each analog can each be uniquely identified by vibrational
 signatures at either ~ 594 cm⁻¹ (R6G-d₄) or ~ 604 cm⁻¹ (R6G),
 as shown in Fig. 7A. By adding spectral resolution to the experiment,
 we can work somewhat above the single molecule level, although we
 have to be careful not to have too many molecules active at a single
 time or the centroid will collapse, as shown in Fig. 4.

45 Fig. 7B shows an example of spectrally-resolved SERS hot
 spot imaging, in which spectral signatures of both R6G and
 R6G-d₄ are observed.²¹ In the early half of the data acquisition,
 both molecules are active with the corresponding spectrum
 showing peaks at both 594 and 604 cm⁻¹. Because both
 emitters are active at the same time, the calculated centroid
 position is an intensity-weighted super-position of the two
 individual plasmon-coupled SERS emission events, as
 described previously. After ~ 50 seconds, we observe a disap-
 50 pearance of the 594 cm⁻¹ peak, suggesting that the R6G-d₄
 either diffused out of the hot spot or photobleached. For the
 remainder of the data acquisition, the centroid shifts to a new

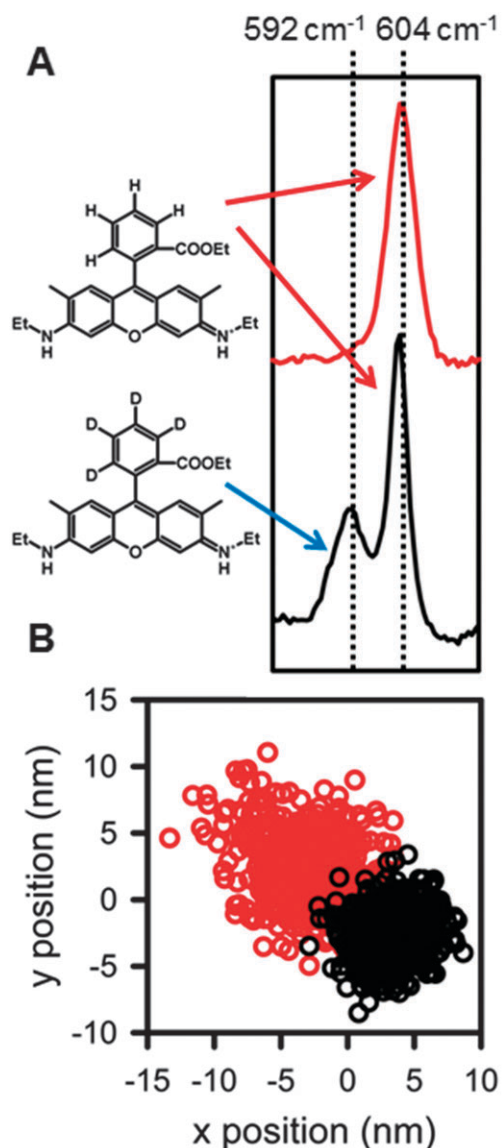


Fig. 7 (A) SERS spectra taken during different times of the data acquisition. In early times (black), spectral signatures of both R6G and R6G-d₄ are observed, while at later times (red), only R6G is observed. (B) Calculated SERS centroid positions for times corresponding to (black) both molecules emitting and (red) only R6G emitting. Adapted with permission from ref. 21. Copyright 2012 American Chemical Society.

location, representing only the plasmon-coupled emission contribution from the R6G molecule. These data prove that the position of the molecule will influence the position of the calculated SERS centroid; if the centroid was dictated exclusively by the geometry of the nanoparticle and not the position of the SERS analyte, then the centroid would not change when the R6G-d₄ molecule ceased emitting. Thus, spectral resolution is important for following how different analytes interact with SERS substrates, especially when working slightly above the SM-SERS level.

Etchegoin and coworkers used a different approach to study SERS hot spots with both spectral and spatial resolution.⁴¹ In their work, the emission from a SERS-active nanoparticle

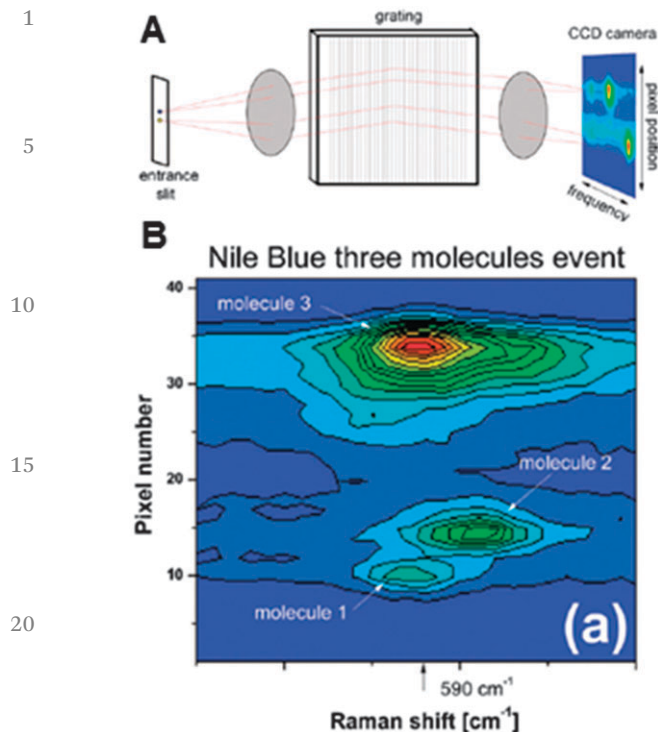


Fig. 8 (A) Schematic of wavelength and spatially resolved SERS imaging, based on reflection of the signal off a grating. Light is spectrally dispersed in the direction orthogonal to the grooves of the grating, providing wavelength resolution on one dimension of the CCD camera, while the other dimension preserves spatial information. (B) Example of spectrally and spatially-resolved emission from a silver nanoparticle aggregate labeled with multiple Nile Blue molecules. Discrete emission sites are observed for three different molecules adsorbed to the aggregate. Reproduced from ref. 36 with permission from the PCCP Owner Societies.

aggregate labeled with Nile Blue molecules was reflected by a grating and then imaged onto a CCD camera. In the direction perpendicular to the grooves of the grating, the angle of reflection off the grating depends on the wavelength of the light; this leads to spectral dispersion of the light onto one dimension of the CCD (the “frequency” dimension, Fig. 8A).⁴¹ On the other hand, if two emitters are spaced from one another along the axis parallel to the grooves of the grating, then their emission will be spatially resolved along the opposite dimension of the CCD (the “pixel” dimension, Fig. 8A). The result is that the CCD contains both spectral and spatial information (along the dimensions perpendicular and parallel to the grooves of the grating, respectively). Although this approach only offers spatial resolution in one dimension, the authors showed that it was possible to spatially resolve emission events from multiple molecules emitting simultaneously, which cannot be done using non-spectrally resolved diffraction-limited imaging (as shown in Fig. 7B, black data). Fig. 8B shows an example in which three Nile Blue molecules are uniquely resolved, based on slight differences between their spectral and spatial profiles. Using spectral data alone, the three emitters cannot be resolved; only by including the additional spatial information does the contribution from each unique emitter become apparent.

Because of optical aberrations introduced by the imaging system, the authors do not pursue sub-diffraction limited resolution in this study (and provide an extensive analysis of their system in the supporting information).⁴¹ However, we hope it is clear to the reader how this approach could have interesting possibilities for future super-resolution SERS hot spot imaging. By integrating spectral and spatial dispersion, the authors have shown a simple strategy for obtaining spatial information while working above the single molecule limit. While challenges remain—notably, overcoming aberration effects in order to fit the data to reasonable point spread function models and obtaining spatial information along more than a single axis—this work is a compelling example of how novel experimental geometries can be designed to yield new insight into SERS hot spots.

As a final example, Yeung and coworkers also used a grating, but in a slightly different geometry, to resolve the spatial and spectral properties of EM hot spots.²⁹ In their experiments, silver spheres are bound to the surface of cysteamine-functionalized silver nanowires, creating multiple hot spots along the length of the nanowire. Next, a dilute solution of Rhodamine B is introduced, and diffraction-limited bursts of fluorescence are observed when a single dye molecule diffuses close enough to a hot spot to be plasmonically-enhanced. To obtain simultaneous spectral resolution, a transmission grating is placed in front of the camera; the zero-order mode of the light transmitted through the grating is used for 2-D Gaussian fitting to obtain centroid localization, while the first-order mode provides wavelength-resolved spectral information. Fig. 9 shows the results of this study, in which two individual hot spots that cannot be resolved in a traditional wide-field image (Fig. 9a) are spatially resolved in the reconstructed image with a distance of ~ 60 nm (Fig. 9b). The two hot spots are labeled “A” and “B,” and the authors find that the intensity of the Rhodamine B emission is stronger from hot spot A than hot spot B. Because the zero-order mode is used for super-resolution centroid determination, the spatial position of the hot spots can be resolved in two dimensions, unlike the previous example shown in Fig. 8.

Using the information from the first-order grating mode, the authors can also measure the emission spectrum of each Rhodamine B molecule as it explores the different hot spots.²⁹ Interestingly, the emission maximum is affected depending on whether the emission is coupled to hot spot A or B. In Fig. 9c, the emission maximum of each fluorescence event is plotted as a function of the calculated centroid position, and the data show that the majority of the fluorescence emission events are red-shifted in hot spot B relative to hot spot A. The authors check whether the emission wavelength is correlated with the intensity (and thus the local EM field enhancement) of the emission and find no correlation; thus the change in the emission wavelength is most likely a combination of the optical properties of the EM hot spot and properties of the molecule itself.

These different examples highlight the power of including wavelength resolution with super-resolution imaging in order

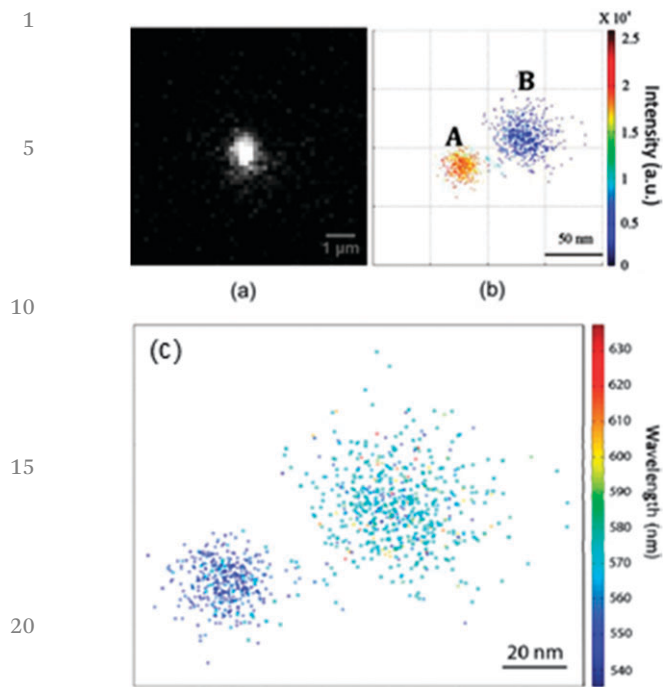


Fig. 9 (a) Diffraction-limited emission from Rhodamine B exploring a hot spot between a silver nanowire and a silver nanosphere. (b) Two discrete hot spots are revealed to be hidden under the diffraction-limited region in (a). The intensity of the Rhodamine B emission events are color coded, showing that hot spot A is more intense than hot spot B. (c) The emission wavelength of the Rhodamine B depends on whether it is coupled to hot spot A or B. Adapted with permission from ref. 27. Copyright 2013 American Chemical Society.

to determine both the identity and number of active SERS tags, as well as provide insight into how the emission energy is coupled out through the plasmon modes of EM hot spots. However, spectral resolution comes at a price: reduced signal-to-noise in the images due to the fact that some fraction of the photons are redirected from the primary diffraction-limited image (as in the example from Fig. 7 and 9) or spectrally dispersed over multiple imaging pixels (as in the example from Fig. 8). As a result, integration times must be increased in order to improve signal-to-noise, in turn reducing temporal resolution. Thus, experiments must be carefully designed to optimize signal-to-noise in both the spectral and spatial dimensions without sacrificing too much information about the dynamics of the system.

6. Conclusions and outlook

In this Tutorial Review, we have explained the basic principles of super-resolution imaging of SERS hot spots and discussed several recent examples that highlight both the power and the associated challenges of this technique. By working at or near the single molecule level, super-resolution imaging allows dynamic changes in the SERS centroid position to be calculated—whether through fitting with a simple 2-D Gaussian or a more complex dipole-based model—and correlated with the

intensity of the SERS signals. These experiments have revealed that the location of the SERS emission depends both on the plasmonic properties of the SERS substrate as well as the location of the emitting analyte on the substrate surface. By exploiting molecular diffusion, we can probe different regions of the SERS substrate, thereby mapping out different local SERS (or fluorescence) intensities and relating these back to plasmonically-enhanced EM fields.

One issue that was not discussed in this review is the ability to perform structural correlation along with super-resolution imaging. By using optically transparent conductive substrates, such as indium tin oxide (ITO) coated coverglass, it is possible to correlate the reconstructed optical images with structural features of the SERS substrate using electron microscopy.^{19,20} To do this, we typically pattern an alphanumeric grid directly onto the ITO coverglass, allowing us to locate the region of interest in both an optical and an electron microscope (the same approach can be used with AFM, although the measured structures have reduced resolution due to AFM tip effects). The fluorescent alignment markers described in Section 2 provide additional features that can be used to positively identify the substrate region of interest. Including structure correlation allows for specific substrate features to be related to locally enhanced EM fields, which is particularly powerful when combined with predictions from theoretical calculations.

The field of super-resolution imaging as applied to plasmonic systems is still in its relative youth, indicating that there remain many exciting experimental challenges and questions to be answered. We have shown several examples in this review of possible directions, such as new fitting models and correlated spectroscopy and imaging, but other options such as three-dimensional super-resolution imaging are also possible.^{42–44} One unique challenge faced in SERS is the fact that we have a coupled emitter based upon a plasmonic substrate and a scattering molecule. This situation is distinct from most super-resolution fluorescence experiments where the emitter is a single radiating dipole. As a result, we must think carefully about how to interpret the results of these experiments given the fact that the emission from the molecule is coupled to the nearby plasmonic substrate.

Even with these challenges, the experiments described here show the power of this technique for mapping out properties of SERS hot spots and understanding the roles of both the molecule and the substrate for defining the emission properties of the hot spot. We have purposefully kept the concepts of EM hot spots and SERS hot spots distinct in this review, because we believe that the two are fundamentally different. While EM hot spots are associated with regions of strongly enhanced EM fields due to the excitation of plasmons by light, SERS hot spots are defined as much by the molecular emitter as they are by the plasmon modes of the substrate. Thus, we must not neglect the role that the molecule can play when designing hot spots for SERS experiments; despite its small size relative to the substrate, super-resolution imaging studies have shown that the molecule can have measurable and important effects in defining SERS hot spots.

Acknowledgements

The author gratefully acknowledges Dr Kyle Marchuk for critical reading of this manuscript. This material is based on work supported by the Welch Foundation under Award No. F-1699.

References

- 1 P. L. Stiles, J. A. Dieringer, N. C. Shah and R. P. Van Duyne, *Annu. Rev. Anal. Chem.*, 2008, **1**, 601.
- 2 E. C. Le Ru and P. G. Etchegoin, *Annu. Rev. Phys. Chem.*, 2012, **63**, 65.
- 3 J. Kneipp, H. Kneipp and K. Kneipp, *Chem. Soc. Rev.*, 2008, **37**, 1052.
- 4 J. R. Lombardi and R. L. Birke, *Acc. Chem. Res.*, 2009, **42**, 734.
- 5 M. Moskovits, *Top. Appl. Phys.*, 2006, **103**, 1.
- 6 K. A. Willets and R. P. Van Duyne, *Annu. Rev. Phys. Chem.*, 2007, **58**, 267.
- 7 B. Ren, G.-K. Liu, X.-B. Lian, Z.-L. Yang and Z.-Q. Tian, *Anal. Bioanal. Chem.*, 2007, **388**, 29.
- 8 M. Fan, G. F. S. Andrade and A. G. Brolo, *Anal. Chim. Acta*, 2011, **693**, 7.
- 9 S. Lal, N. K. Grady, J. Kundu, C. S. Levin, J. B. Lassiter and N. J. Halas, *Chem. Soc. Rev.*, 2008, **37**, 898.
- 10 A. L. Lereu, A. Passian and P. Dumas, *Int. J. Nanotechnol.*, 2012, **9**, 488.
- 11 E. Ringe, B. Sharma, A.-I. Henry, L. D. Marks and R. P. Van Duyne, *Phys. Chem. Chem. Phys.*, 2013, **15**, 4110.
- 12 K. A. Willets, *Prog. Surf. Sci.*, 2012, **87**, 209.
- 13 L. Brus, *Acc. Chem. Res.*, 2008, **41**, 1742.
- 14 S. L. Kleinman, R. R. Frontiera, A.-I. Henry, J. A. Dieringer and R. P. Van Duyne, *Phys. Chem. Chem. Phys.*, 2013, **15**, 21.
- 15 K. A. Willets, S. M. Stranahan and M. L. Weber, *J. Phys. Chem. Lett.*, 2012, **3**, 1286.
- 16 A. M. Michaels, J. Jiang and L. Brus, *J. Phys. Chem. B*, 2000, **104**, 11965.
- 17 S. M. Stranahan and K. A. Willets, *Nano Lett.*, 2010, **10**, 3777.
- 18 H. Cang, A. Labno, C. Lu, X. Yin, M. Liu, C. Gladden, Y. Liu and X. Zhang, *Nature*, 2011, **469**, 385.
- 19 M. L. Weber and K. A. Willets, *J. Phys. Chem. Lett.*, 2011, **2**, 1766.
- 20 M. L. Weber, J. P. Litz, D. J. Masiello and K. A. Willets, *ACS Nano*, 2012, **6**, 1839.
- 21 E. J. Titus, M. L. Weber, S. M. Stranahan and K. A. Willets, *Nano Lett.*, 2012, **12**, 5103.
- 22 C. Coltharp and J. Xiao, *Cell. Microbiol.*, 2012, **14**, 1808.
- 23 W. E. Moerner, *J. Microsc.*, 2012, **246**, 213.
- 24 J. Steidtner and B. Pettinger, *Phys. Rev. Lett.*, 2008, **100**, 236101.
- 25 B. Pettinger, *Mol. Phys.*, 2010, **108**, 2039.
- 26 K. A. Willets, *Phys. Chem. Chem. Phys.*, 2013, **15**, 5345.
- 27 W. E. Moerner and D. P. Fromm, *Rev. Sci. Instrum.*, 2003, **74**, 3597.
- 28 R. E. Thompson, D. R. Larson and W. W. Webb, *Biophys. J.*, 2002, **82**, 2775.
- 29 L. Wei, C. Liu, B. Chen, P. Zhou, H. Li, L. Xiao and E. S. Yeung, *Anal. Chem.*, 2013, **85**, 3789.
- 30 L. K. Ausman and G. C. Schatz, *J. Chem. Phys.*, 2009, **131**, 084708.
- 31 C. E. Talley, J. B. Jackson, C. Oubre, N. K. Grady, C. W. Hollars, S. M. Lane, T. R. Huser, P. Nordlander and N. J. Halas, *Nano Lett.*, 2005, **5**, 1569.
- 32 E. J. Titus and K. A. Willets, *ACS Nano*, 2013, DOI: 10.1021/nn403891t.
- 33 K. I. Mortensen, L. S. Churchman, J. A. Spudich and H. Flyvbjerg, *Nat. Methods*, 2010, **7**, 377.
- 34 J. Engelhardt, J. Keller, P. Hoyer, M. Reuss, T. Staudt and S. W. Hell, *Nano Lett.*, 2011, **11**, 209.
- 35 J. Enderlein, E. Toprak and P. R. Selvin, *Opt. Express*, 2006, **14**, 8111.
- 36 S. M. Stranahan, E. J. Titus and K. A. Willets, *J. Phys. Chem. Lett.*, 2011, **2**, 2711.
- 37 S. M. Stranahan, E. J. Titus and K. A. Willets, *ACS Nano*, 2012, **6**, 1806.
- 38 A. P. Bartko and R. M. Dickson, *J. Phys. Chem. B*, 1999, **103**, 11237.
- 39 E. J. Titus and K. A. Willets, *ACS Nano*, 2013, **7**, 6258.
- 40 J. Lippincott-Schwartz and S. Manley, *Nat. Methods*, 2009, **6**, 21.
- 41 P. G. Etchegoin, R. E. C. Le and A. Fainstein, *Phys. Chem. Chem. Phys.*, 2011, **13**, 4500.
- 42 B. Huang, W. Wang, M. Bates and X. Zhuang, *Science*, 2008, **319**, 810.
- 43 B. Huang, *Nat. Methods*, 2011, **8**, 304.
- 44 S. R. P. Pavani, M. A. Thompson, J. S. Biteen, S. J. Lord, N. Liu, R. J. Twieg, R. Piestun and W. E. Moerner, *Proc. Natl. Acad. Sci. U. S. A.*, 2009, **106**, 2995.